Alternative path for bridging the A = 5, 8 gap in neutron-rich nucleosynthesis scenarios

R de Diego, E Garrido, D V Fedorov, a S Jensen

Alternative path for bridging the A=5,8 gap in neutron-rich nucleosynthesis scenarios

R de Diego[1], E Garrido[1], D V Fedorov[1], and A S Jensen[1]

[1] Instituto de Estructura de la Materia, CSIC, Serrano 123, E-28006 Madrid, Spain
[2] Department of Physics and Astronomy, University of Aarhus, DK-8000 Aarhus C, Denmark

Abstract. In neutron-rich nucleosynthesis scenarios the mass gaps A=5,8 are assumed to be bridged by the three-body electromagnetic recombination reaction ^{4}He$(\alpha n,\gamma)^9$Be. However an alternative path, the nuclear four-body neutron-recoil recombination reaction ^{4}He$(\alpha nn,n)^9$Be, is also conceivable in neutron-rich environments. We estimate the rate of the alternative reaction and show that for temperatures of about 10^9K it is comparable with the electromagnetic rate if the neutron density is of about 10^{30} neutrons per cm^3. At higher neutron densities the nuclear process dominates.

Keywords r-process, neutron-rich stellar environments

1. Introduction

In neutron-rich scenarios of astrophysical nucleosynthesis heavy elements are formed by rapid neutron capture in hot neutron-rich environments with 10^{20-30} neutrons per cm^3 and temperatures of about 10^9K [1, 2]. The recombination of two α-particles and a neutron into ^{9}Be nucleus plays a key role in these scenarios as it bridges the gaps of unstable isotopes with mass numbers A=5 and A=8 [3]. The recombination is assumed to occur through the three-body electromagnetic reaction,

$$^4\mathrm{He}(\alpha n,\gamma)^9\mathrm{Be}\,, \tag{1}$$

where the excess energy is taken away by the emitted photon [3, 4, 5, 6].

However in neutron-rich environments the recombination can also occur through the nuclear four-body neutron-recoil recombination reaction

$$^4\mathrm{He}(\alpha nn,n)^9\mathrm{Be}\,, \tag{2}$$

where the excess energy is passed to a neutron in the environment.

In this letter we estimate the production rate of ^{9}Be from the neutron-recoil recombination reaction (2) for different temperatures of the environment and compare it with the rate of the electromagnetic reaction (1).

2. Neutron-recoil recombination

We shall describe the nuclear recombination reaction (2) using the participant-spectator model [7] where the recombining three-body $\alpha\alpha n$ system (participants) is treated rigorously while the recoil neutron (spectator) is accounted for in the plane-wave approximation.

In this model the transition amplitude M_{fi} for the recombination of the $\alpha\alpha n$ system from an initial (continuum) three-body state $|i\rangle$ to the final (bound) three-body state $\langle f|$ is given as

$$M_{fi} = \int d^3r \langle f| \frac{e^{-i\boldsymbol{p}'\cdot\boldsymbol{r}}}{\sqrt{V}} W \frac{e^{+i\boldsymbol{p}\cdot\boldsymbol{r}}}{\sqrt{V}} |i\rangle \ , \tag{3}$$

where $\boldsymbol{r}$ is the relative coordinate between the recoil-neutron and the $\alpha\alpha n$ center of mass, $\boldsymbol{p}$ and $\boldsymbol{p}'$ are the initial and final momenta of the recoil neutron (relative to the $\alpha\alpha n$ system), and W is the interaction between the recoil neutron and the $\alpha\alpha n$ system.

We shall use the box boundary condition where the three-body states $|i\rangle$ are normalized to unity within the volume V. The continuum states are then discretized, which simplifies the numerical calculations. The final results should be independent of the choice of the volume as long as it is larger than the typical volume of the $\alpha\alpha n$ bound state.

Temperatures of about 10^9 K correspond to neutron kinetic energy around 0.1 MeV, which is small on the scale of neutron-neutron and neutron-α scattering. In this low-energy regime the scattering processes are determined primarily by the corresponding scattering lengths. However, the singlet neutron-neutron scattering length, $a_{nn} \sim 20$ fm is about ten times larger than the neutron-α scattering length. Therefore we shall neglect the neutron-α interaction in the matrix element (3) and include only the neutron-neutron interaction.

In the low-energy regime the neutron-neutron interaction can be approximated by the Fermi's pseudo-potential, particularly suitable for the plane-wave approximation,

$$W = \frac{4\pi\hbar^2 a_{nn}}{m} \delta(\boldsymbol{r}_{nn}) \ , \tag{4}$$

where $\boldsymbol{r}_{nn}$ is the distance between the two neutrons and m is the neutron mass.

Introducing $\boldsymbol{r}_n = \boldsymbol{r} - \boldsymbol{r}_{nn}$ as the coordinate between the recombining neutron and the center of mass of the recombining $\alpha\alpha n$ system, and integrating (3) with the δ-function (4) we obtain

$$M_{fi} = \frac{4\pi\hbar^2 a_{nn}}{Vm} \langle f| e^{-i\boldsymbol{q}\cdot\boldsymbol{r}_n} |i\rangle \ , \tag{5}$$

where $\boldsymbol{q} = \boldsymbol{p}' - \boldsymbol{p}$ is the transferred momentum. The two neutrons here are assumed to be in the singlet state.

Since the temperature of the environment is much smaller than the binding energy of ^{9}Be we neglect the initial thermal energy of the system compared to the recoil energy. Neglecting also the mass of the neutron compared to the mass of ^{9}Be, we assume that

for all initial states the recoil energy is equal to the binding energy of ^{9}Be, called ϵ, and thus

$$q = p' = \sqrt{\frac{2m\epsilon}{\hbar^2}} \, . \tag{6}$$

Assuming there are N_n recoil neutrons available in the volume V, the differential probability (the number of transitions per unit time) for the transition $|i\rangle \to |f\rangle$ for one $\alpha\alpha n$ system is given by the Fermi's Golden rule,

$$dw_{fi} = \frac{N_n}{4} \frac{2\pi}{\hbar} |M_{fi}|^2 \frac{d\nu_q}{dE_q} \, , \tag{7}$$

where the factor 1/4 is the probability to find two neutrons in a singlet state in a thermal gas of neutrons, and where $d\nu_q$ is the number of states per unit energy for the recoil neutron, given by

$$d\nu_q = \frac{V d^3q}{(2\pi)^3} = \frac{qmV}{(2\pi)^3\hbar^2} d\Omega_q dE_q \, , \tag{8}$$

where $d\Omega_q$ is an infinitesimal solid angle around the direction of q and E_q is the energy of the recoil neutron.

Substitution the matrix element (5) and the number of states (8) into (7) gives

$$dw_{fi} = n_n a_{nn}^2 v \left| \langle f | e^{-i\boldsymbol{q}\cdot\boldsymbol{r}_n} | i \rangle \right|^2 d\Omega_q \, , \tag{9}$$

where $n_n = N_n/V$ is the neutron density and $v = \hbar q/m$ is the final velocity of the recoil neutron.

After integration over the recoil angles, summing over the final magnetic quantum numbers μ_f, and averaging over the initial ones μ_i, we get the reaction rate

$$w_{fi} = n_n a_{nn}^2 v F_{fi} \, , \tag{10}$$

where

$$F_{fi} = \frac{1}{(2j_i+1)} \sum_{\mu_f \mu_i} \int d\Omega_q \left| \langle j_f \mu_f | e^{-i\boldsymbol{q}\cdot\boldsymbol{r}_n} | j_i \mu_i \rangle \right|^2 \tag{11}$$

and j_i, j_f are the angular momenta of the initial and the final states.

The quantity F_{fi} depends on the normalization volume V for the three-body states. However, the probability per unit energy

$$\frac{dw}{dE} = n_n a_{nn}^2 v \frac{dF}{dE} \, , \tag{12}$$

where the nuclear strength function $\frac{dF}{dE}$ is given as

$$\frac{dF}{dE} = \frac{1}{\Delta E} \sum_{E_i \in E \pm \Delta E/2} F_{fi} \, , \tag{13}$$

is independent on the normalization volume.

In practice the energy bin ΔE should be chosen small enough for not to smear out the structure of the spectrum, but still large enough to include several discretized continuum states in each energy bin.

3. Electromagnetic recombination

The dipole electromagnetic recombination reaction rate is given as [8]

$$w_{fi}^{(E1)} = 8\pi \frac{2}{9} \frac{\omega^3}{\hbar c^3} B_{fi}^{(E1)} \tag{14}$$

where $\hbar\omega$ is the photon energy, and $B_{fi}^{(E1)}$ is the reduced dipole transition probability integrated over the photon angles and summed over magnetic quantum numbers of the final state,

$$B_{fi}^{(E1)} = 4(2e)^2 \sum_{\mu\mu_f} |\langle j_f \mu_f | r_\alpha Y_{1\mu}(\boldsymbol{r}_\alpha) | j_i \mu_i \rangle|^2 \,, \tag{15}$$

where $\boldsymbol{r}_\alpha$ is the coordinate of an α-particle from the center of mass of the recombining $\alpha\alpha n$ system, $2e$ is the charge of the α-particle, and the factor of 4 appears because the system contains two identical α-particles.

We can rewrite the reaction rate (14) in a more elucidating form as

$$w_{fi}^{(E1)} = \frac{(4\pi)^3}{9} \omega \frac{e^2}{\hbar c} \left(\frac{R}{\lambda}\right)^2 \frac{B_{fi}^{(E1)}}{e^2 R^2} \tag{16}$$

where R ($\approx$ 2.52 fm) is the root mean square charge radius of ^{9}Be, and λ is the wavelength of the photon.

Similarly to (12) we introduce the electromagnetic rate per unit energy,

$$\frac{dw^{(E1)}}{dE} = \frac{(4\pi)^3}{9} \omega \frac{e^2}{\hbar c} \left(\frac{R}{\lambda}\right)^2 \frac{dF^{(E1)}}{dE} \tag{17}$$

where the reduced electromagnetic strength function,

$$\frac{dF^{(E1)}}{dE} = \frac{1}{\Delta E} \sum_{E_i \in E \pm \Delta E/2} \frac{B_{fi}^{(E1)}}{e^2 R^2} \,, \tag{18}$$

is independent of the size of the normalization volume.

Note that only the initial states that satisfy the dipole transition selection rules in (15) are included in the electromagnetic sum (18) while the nuclear sum (11) includes, in principle, states with all angular momenta. This might be important for higher energies of the initial states.

4. Temperature

In an environment with temperature T the probability to find a system in a state with energy E_i is given by the Boltzmann distribution,

$$P_i = g_i \frac{e^{\frac{-E_i}{k_B T}}}{Z} \,, \; Z \equiv \sum_i g_i e^{\frac{-E_i}{k_B T}} \,, \tag{19}$$

where g_i is the degeneracy factor of the state i, and k_B is the Boltzmann constant.

The total recombination rate $\langle \alpha\alpha n \rangle_\gamma$ is then the Boltzmann averaged sum of the contributions from all possible initial states or, equivalently, the Boltzmann integral over

the energy of the initial state over the nuclear (12) or electromagnetic (17) differential rates,

$$\langle \alpha\alpha n \rangle = \sum_i g_i \frac{e^{\frac{-E_i}{k_B T}}}{Z} w_{fi} = \int_0^\infty dE \frac{e^{\frac{-E}{k_B T}}}{Z} \frac{dw}{dE} \ . \tag{20}$$

The degeneracy factor g_i is included in dw/dE through the summation over all the states inside each energy bin in (13) and (18).

In order to calculate the partition function Z via the summation (19) a large number of continuum states with different parities and total momenta needs to be calculated. To simplify the calculations we shall use the partition function for a free $\alpha\alpha n$ system where the interactions between particles are neglected.

The partition function of a system can be expressed as an integral,

$$Z = \int_0^\infty dE \ g(E) e^{\frac{-E}{k_B T}} \ , \tag{21}$$

where $g(E)$ is the density of states of the system. For a free $\alpha\alpha n$ system the density of states is given as

$$g(E) = \frac{4(\mu_{\boldsymbol{x}}\mu_{\boldsymbol{y}})^{\frac{3}{2}} V_6 \pi^3 E^2}{(2\pi\hbar)^6} \ , \tag{22}$$

where μ_x and μ_y are the reduced masses associated to the Jacobi coordinates $\boldsymbol{x}$ and $\boldsymbol{y}$, and V_6 is the six-dimensional volume, which in terms of the hyperradius $\rho = \sqrt{x^2 + y^2}$ takes the form:

$$V_6 = \frac{\pi^3 \rho_{max}^6}{6} \ , \tag{23}$$

with ρ_{max} being the size of the box used to discretize the three-body continuum spectrum.

5. Numerical results

The three-body wave functions for the $\alpha\alpha n$ system have been obtained by means of the hyper-spherical adiabatic expansion method [9]. The details of the interaction can be found in [10] and [11]. We have used a box boundary condition at $\rho_{max} \sim 100$ fm which converts the continuum spectrum into a discretized quasi-continuum. The size of the energy bin (ΔE) in the summations (13) and (18) is chosen about 0.2 MeV, such that each of them contains eight quasi-continuum states. After binning an interpolation procedure is used to obtain a smooth function.

In Fig. 1 we show the nuclear (13) and electromagnetic (18) strength functions as a function of the energy of the initial state. The low-lying peak in the strength functions has been obtained using a Breit-Wigner interpolation function centered at the resonance energy of 0.14 MeV with the width of 0.11 MeV. These parameters are from the analysis in [12], where this resonance was interpreted as a genuine three-body structure owing its finite lifetime to substantial restructuring from small to large distances. This is an important point, since this determines the behavior of the strength functions at very low

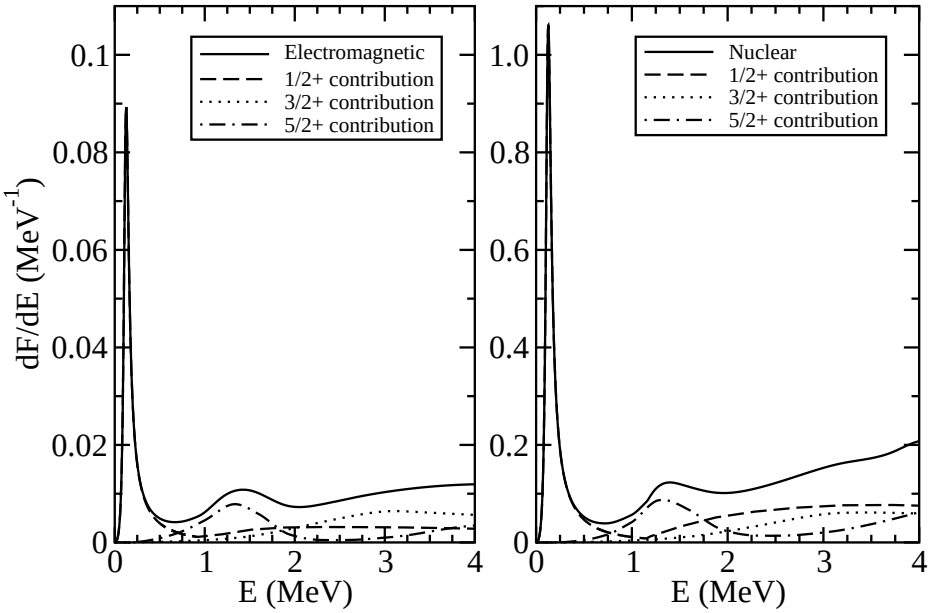

Figure 1. Electromagnetic strength function (18) (left) and nuclear strength function (13) (right) for the $\alpha\alpha n \rightarrow {}^{9}$Be recombination process as a function of the energy of the initial state.

energy where our discretization procedure gives too few points. The low-temperature dependence is in turn determined by this parametrized low-energy behavior‡.

The nuclear rate has been computed using the same continuum states as for the electromagnetic dipole rate, that is continuum states with total momentum and parity $1/2^+$, $3/2^+$, and $5/2^+$. The strength functions reflect the resonant structure of the $\alpha\alpha n$ system in the corresponding channels.

Both strengths contain only quantities of the natural scale of the three-body system and reflect the resonant structure of the $\alpha\alpha n$ continuum. The main difference between them arises from the operators in the matrix elements (11) and (15). Although similar in the dipole approximation they depend on r_n and r_α in (11) and (15), respectively. The fact that the nuclear strength is bigger than the electromagnetic one is a sign of the larger average distance from the three-body center of mass of the neutron compared to that of the alpha particle.

In Fig. 2 we show the Boltzmann averaged recombination rates (per one $\alpha\alpha n$ system) as function of temperature. In the left part of the figure the closed and open squares correspond to the rates obtained in [6] and [14], respectively. In [6] the rate is derived in the sequential approximation through the metastable 0^+ state in ^{8}Be. The $1/2^+$, $5/2^-$ and $5/2^+$ states in ^{9}Be are included. The same formulation as in [15] is used, and actually very similar results are obtained. The energy of 0.161 MeV above

‡ in ref.[13] the low-energy behavior of the ^{9}Be ($\frac{1}{2}^+ \rightarrow \frac{3}{2}^-$) contribution was inadvertently incorrectly treated and the resulting low-temperature rate was therefore incorrect. In this paper we use the proper interpolation procedure at low energies and the resulting rates are shown in figure 2. The conclusions in [13] are unaltered although the detailed rate dependence at low temperatures is now substantially improved.

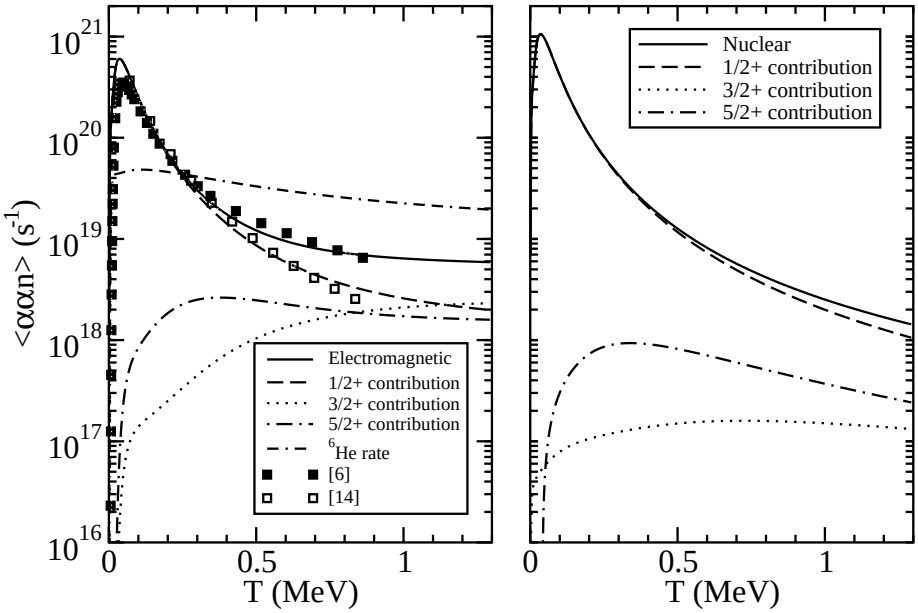

Figure 2. Boltzmann averaged electromagnetic (left) and nuclear (right) rates for the $\alpha\alpha n \rightarrow {}^9$Be recombination. The closed and open squares on the left part are the results from [6] and [14]. The dash-dash-dot curve on the left part is the rate for the $\alpha nn \rightarrow {}^6\mathrm{He} + \gamma$ recombination reaction, given here for comparison. The nuclear rate is calculated for the neutron density $\check{n}_n = 10^{30}\mathrm{cm}^{-3}$. Since the nuclear rate (10) is proportional to the neutron density, the rate for a given neutron density n_n can be obtained by rescaling the curves with the factor $n_n/\check{n}_n$.

the three-body threshold and the width of 0.225 MeV is used for the low-lying $1/2^+$ state in ^{9}Be. In the previous work [14] the photodissociation cross section for ^{9}Be is adjusted with a simple exponentially falling function, which basically only reproduces the low lying $1/2^+$ peak. As seen in the figure, the full calculation (solid line) agrees reasonably well with the results in [6], while the contribution of the $1/2^+$ states (dashed line) agrees with [14], where essentially only that state is considered. This agreement can be understood from the fact that the main contribution to the rate comes from the $\alpha\alpha n$ states with spin and parity $1/2^+$ (dashed line), which is to a large extent dominated by the $1/2^+$ resonance in ^{9}Be. The full three-body calculation predicts that this resonance decays almost fully sequentially through the 0^+ state in ^{8}Be. Therefore, the population of the resonance (which is the inverse process) should mainly proceed sequentially through the 0^+ state in ^{8}Be, precisely as assumed in [6].

Another process leading to ^{9}Be is the α-capture on ^{6}He, i.e., the $\alpha(nn,\gamma)^6\mathrm{He}(\alpha,n)^9\mathrm{Be}$ process. We then for comparison show in the left part of figure 2 the electromagnetic recombination rate obtained by means of a full three-body calculation for the $\alpha nn \rightarrow {}^6\mathrm{He} + \gamma$ reaction (dash-dash-dot curve). At small temperatures the ^{9}Be rate clearly dominates. This is due to the low-lying $1/2^+$ resonance in ^{9}Be. Only for temperatures around 0.3 MeV (~ 3.5 GK) the ^{6}He rate is taking over.

The nuclear rate was calculated for a neutron density of $\check{n}_n = 10^{30}$ cm^{-3}. At this density the nuclear and electromagnetic rates are comparable at temperatures of few

GK. The nuclear rate (10) is proportional to the neutron density, therefore the nuclear rate for a given neutron density n_n can be obtained from the curves on Fig. 2 (right) by rescaling with the factor $n_n/\check{n}_n$.

6. Conclusion

We have investigated an alternative path for bridging the gap of unstable nuclear isotopes with A=5,8 in neutron-rich nucleosynthesis scenarios. The alternative path is the nuclear four-body recombination reaction $^4\mathrm{He}(\alpha nn, n)^9\mathrm{Be}$. We have estimated the rate of the nuclear recombination using the participant-spectator model and compared it with the rate of the electromagnetic recombination reaction $^4\mathrm{He}(\alpha n, \gamma)^9\mathrm{Be}$. We have shown that for scenarios with a neutron density of the order of 10^{30} cm^{-3} both rates are comparable at a temperature of 10^9 K. At higher neutron densities the nuclear process dominates.

Acknowledgments. This work was partly supported by funds provided by DGI of MEC (Spain) under contract No. FIS2008-01301. One of us (R.D.) acknowledges support by a Ph.D. I3P grant from CSIC and the European Social Fund.

References

[1] B.S. Meyer, G.J. Mathews, W.M. Howard, S.E. Woosley, and R.D. Hoffman, Astrophys. J. **399**, 656 (1992).
[2] J.J. Cowan, and F.-K. Thielemann, Phys. Today 57 (2004) 47-53
[3] V.D. Efros, H. Oberhummer, A. Pushkin, and I.J. Thompson, Eur. Phys. J. **A1** 447 (1998).
[4] J. Görres, H. Herndl, I.J. Thompson, and M. Wiescher, Phys. Rev. **C52**, 2231 (1995).
[5] A. Bartlett, J. Görres, G.J. Mathews, K. Otsuki, M. Wiescher, D. Frekers, A. Mengoni, and J. Tostevin, Phys. Rev. **C74**, 015802 (2006).
[6] K. Sumiyoshi, H. Utsunomiya, S. Goko, and T. Kajino, Nucl. Phys. **A709**, 467 (2002).
[7] E. Garrido, D.V. Fedorov, and A.S. Jensen, Nucl. Phys. **A695**, 109 (2001).
[8] P.J. Siemens, and A.S. Jensen, Elements of Nuclei, Addison-Wesley, 1987, ISBN 0-201-15572-9
[9] E. Nielsen, D.V. Fedorov, A.S. Jensen, and E. Garrido, Phys. Rep. **347**, 373 (2001).
[10] E. Garrido, D.V. Fedorov, A.S. Jensen, Nucl. Phys. A 700, 117 (2002).
[11] R. Alvarez-Rodriguez, E. Garrido, A.S. Jensen, D.V. Fedorov, and H.O.U. Fynbo, Eur.Phys.J. A 31, 303 (2007).
[12] E. Garrido, D.V. Fedorov, A.S. Jensen, Phys. Lett. B 684, 132 (2010).
[13] R. de Diego, E. Garrido, D.V. Fedorov, and A.S. Jensen, Europhys. Lett. **90**, 52001 (2010).
[14] G.R. Caughlan and W.A. Fowler, At. Data Nucl. Data Tables 40, 283 (1988).
[15] C. Angulo et al., Nucl. Phys. A 656, 3 (1999).